

Not All Tokens and Heads Are Equally Important: Dual-Level Attention Intervention for Hallucination Mitigation

Lexiang Tang, Xianwei Zhuang, Bang Yang, Zhiyuan Hu, Hongxiang Li, Lu Ma, Jinghan Ru, Yuexian Zou*

Peking University, China

{tanglexiang, xwzhuang, huzhiyuan, lihongxiang, maluqax, rujinghan}@stu.pku.edu.cn {yangbang, zouyx}@pku.edu.cn

Abstract

Large vision-language models (LVLMs) have shown remarkable capabilities across a wide range of multimodal tasks. However, they remain prone to visual hallucination (VH), often producing confident but incorrect descriptions of visual content. In this work, we present VisFlow, an efficient and training-free framework designed to mitigate VH by directly manipulating attention patterns during inference. Through systematic analysis, we identify three key pathological attention behaviors in LVLMs: (1) Weak visual grounding, where attention to visual tokens is both insufficient and misallocated, over focusing on visually uninformative tokens or the trailing areas of the image; (2) Language prior dominance, where excessive attention to prior response tokens reinforces autoregressive patterns and compromises multimodal alignment; (3) Prompt redundancy, where numerous attention heads assign abnormally high weights to system prompt tokens, inhibiting the integration of visual, instruction, and response content. To address these issues, we propose two effective interventions: Token-level Attention Intervention (TAI) to enhance attention to salient visual content, and Head-level Attention Intervention (HAI) suppresses over-attention to system prompt tokens and adjacent text tokens, thereby enhancing visual grounding and mitigating the model’s over-reliance on linguistic priors encoded in textual inputs. Extensive experiments across multiple models and benchmarks demonstrate that VisFlow significantly reduces hallucinations and improves visual factuality, all while incurring negligible computational overhead.

Introduction

Riding on the rapid advancement of Large Language Models (LLMs)(Touvron et al. 2023; Chiang, Li et al. 2023; Touvron et al. 2023; Ru et al. 2025), Large Vision-Language Models (LVLMs)(Chen et al. 2023b; Liu et al. 2023; Ye et al. 2024; Bai et al. 2023; Chen et al. 2024a; Li et al. 2023a; Chen et al. 2023a; Zhuang et al. 2025a) have demonstrated remarkable performance across a wide range of multimodal understanding and generation tasks. Typically, the LLM component of an LVLM takes as input several types of tokens: (1) System tokens, which provide high-level configuration or behavior instructions; (2) Visual tokens, which encode the image content; (3) Instruction tokens, which describe user queries or

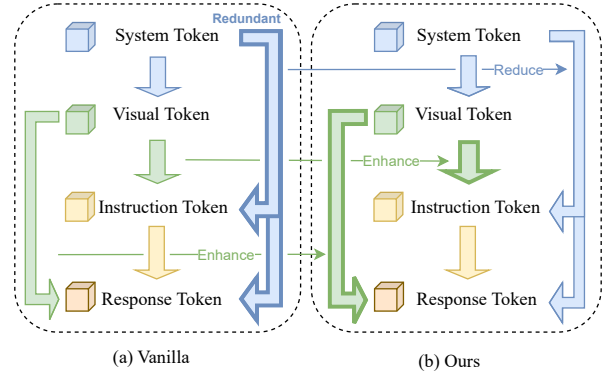


Figure 1: Comparison of token-level information flow before and after attention intervention. The left side illustrates vanilla attention interactions, where visual tokens receive suppressed focus due to over-attention on system prompts. The right side shows VisFlow-modified flows, highlighting enhanced visual factuality and balanced attention allocation.

commands. Based on these, the model generates response tokens as its textual output.

Despite impressive capabilities, LVLMs are prone to generating content that is inconsistent or contradictory to the visual input, a phenomenon referred to as Visual Hallucination (VH) (Liu et al. 2024b; Leng et al. 2024; Huang et al. 2024). VH undermines trust and limits LVLMs’ utility in real-world or safety-critical applications. Existing approaches to VH mitigation fall into three main categories: Post-processing and self-correction (Manakul, Liusie, and Gales 2023; Yin et al. 2024), Instruction-tuning with hallucination-aware data (Ma et al. 2024; Jiang et al. 2024; Sarkar et al. 2024), Decoding-time intervention (Huang et al. 2024; Chen et al. 2024b; Zhuang et al. 2025b). While post-processing and tuning approaches may improve factuality, they often require costly data collection, re-training, or additional inference with large expert models. Decoding-based methods are typically training-free, but many rely on external grounding tools or multi-round reranking, leading to latency overhead.

In this work, we propose VisFlow, a training-free, plug-and-play inference-time strategy that proactively mitigates VH by directly reshaping token-level and head-level atten-

*Corresponding author: Yuexian Zou.

tion flow in the decoder of LVLMs. Our systematic analysis of decoder attention in LVLMs reveals three key patterns associated with hallucination: (1) Weak visual grounding: Attention is inaccurately distributed and often neglects salient visual tokens, leading to vague or visually unanchored responses; (2) Language prior dominance: Attention over-concentrates on the most recent response tokens, impairing multimodal alignment. (3) Prompt redundancy: Many attention heads allocate excessive attention to system prompt tokens, disrupting the integration of image, instruction, and response content. To address these issues, we introduce two core components within VisFlow: Token-Level Attention Intervention (TAI), which strengthens the attention to salient visual regions based on cross-modal saliency analysis; Head-Level Attention Intervention (HAI), which suppresses attention heads identified via causal probing as disproportionately focusing on system prompt tokens or nearby text tokens, both of which are correlated with VH. Unlike contrastive decoding (Huang et al. 2024; Jiang et al. 2024), VisFlow does not rerank outputs or increase decoding steps.

Our Contributions

- We analyze visual hallucination in LVLMs through the lens of attention distribution and information flow, identifying two types of visual tokens and three types of attention heads strongly associated with hallucination.
- We introduce VisFlow, a training-free and efficient inference-time framework incorporating Token-Level and Head-Level Attention Interventions to enhance visual grounding and suppress hallucinations.
- Comprehensive experiments demonstrate that VisFlow substantially outperforms existing visual hallucination mitigation methods in both effectiveness and efficiency.

RELATED WORK

Large Vision-Language Model. Large vision-language models (LVLMs) combine large language models (LLMs) with visual encoders to handle multimodal inputs. Early approaches, such as the LLaVA series (Liu et al. 2024a, 2023), align visual features with LLMs via linear projections and enhance performance through instruction tuning. Other works like BLIP-2 (Li et al. 2023a), MiniGPT-4 (Chen et al. 2023a), and InstructBLIP (Liu et al. 2023) introduce query transformers (e.g., Q-former (Li et al. 2023a)) to extract instruction-aware visual features for improved efficiency. Recent models such as Qwen-VL (Bai et al. 2023), mPLUG-Owl2 (Ye et al. 2024), and InternVL (Chen et al. 2024a) further optimize architectures, training, and data pipelines.

Visual Hallucination Mitigation. Existing efforts to mitigate visual hallucination (VH) in LVLMs fall into three categories: (1) *Instruction tuning* (Gunjal, Yin, and Bas 2024; Ma et al. 2024; Jiang et al. 2024), which improves grounding but requires task-specific data and costly training; (2) *Auxiliary analysis* (Manakul, Liusie, and Gales 2023; Chen et al. 2024b; Yin et al. 2024; An et al. 2024), which adds inference-time modules for hallucination detection at the cost of latency and complexity; and (3) *Decoding strategies* (Leng et al. 2024; Chuang et al. 2023; Huang et al. 2024; Zhuang et al. 2024), which modify generation but may

cause semantic drift. In contrast, we propose VISFLOW, a training-free, efficient approach that intervenes in attention mechanisms at inference by identifying salient visual tokens and critical attention heads to suppress VH without sacrificing speed or requiring extra components.

Tracing information flow in MLLMs. A recent study by Zhang et al. (Zhang et al. 2024) provides the first empirical visualization of cross-modal information flow in the decoder of LVLMs, revealing a three-stage process: (1) shallow layers integrate global visual features into question tokens; (2) mid-level layers selectively align localized visual regions to relevant questions; and (3) deep layers transfer accumulated visual information from question tokens to output tokens. However, this work does not analyze the interaction among visual tokens themselves, a gap we address by intervening in visual-visual token communication. Furthermore, our work is related to CCA-LLaVA (Xing et al. 2024), which has analyzed visual hallucination from the perspective of disrupted token-level information flow particularly due to the long-term decay in RoPE between visual and instruction tokens. builds upon these insights we takes a further step by explicitly modeling and modifying information flow to mitigate VH.

METHOD

This section analyzes token-level information flow and attention distribution in MLLMs, and introduces our dual-level intervention methods.

Measuring the information flow between three type of tokens. To analyze how MLLMs utilize visual information and why they may overly rely on language priors, we adopt the saliency technique (Simonyan, Vedaldi, and Zisserman 2013), a widely used interpretation tool, to highlight critical token interactions within the attention mechanism. Specifically, we apply Taylor expansion to compute the saliency score for each attention matrix element as:

$$I_l = \left| \sum_h A_{h,l} \odot \frac{\partial \mathcal{L}(x)}{\partial A_{h,l}} \right|, \quad (1)$$

where $A_{h,l}$ denotes the attention matrix from the h -th head in the l -th layer, and $\mathcal{L}(x)$ is the task loss. The saliency matrix I_l is obtained by aggregating across all heads to quantify the importance of attention links. Each element $I_l(i, j)$ reflects the contribution of token j to token i in layer l .

To quantify the directional flow of information between different token groups (e.g., system, visual, textual), we define a unified metric:

$$S_{ab} = \frac{\sum_{(i,j) \in C_{ab}} I(i, j)}{|C_{ab}|}, \quad (2)$$

$$C_{ab} = \{(i, j) : i \in \mathcal{A}, j \in \mathcal{B}\} \quad (3)$$

where $I(i, j)$ denotes the information flow from token j to token i , and C_{ab} is the set of directed token pairs from source group \mathcal{B} to target group \mathcal{A} . The sets \mathcal{A} and \mathcal{B} represent token types of interest, such as S_{sv} ($\mathcal{A} = \text{vis}$, $\mathcal{B} = \text{sys}$), S_{vv} ($\mathcal{A} = \mathcal{B} = \text{vis}$, with optional constraint $i \geq j$), and S_{vt} ($\mathcal{A} = \text{txt}$, $\mathcal{B} = \text{vis}$). This metric provides a normalized estimate of

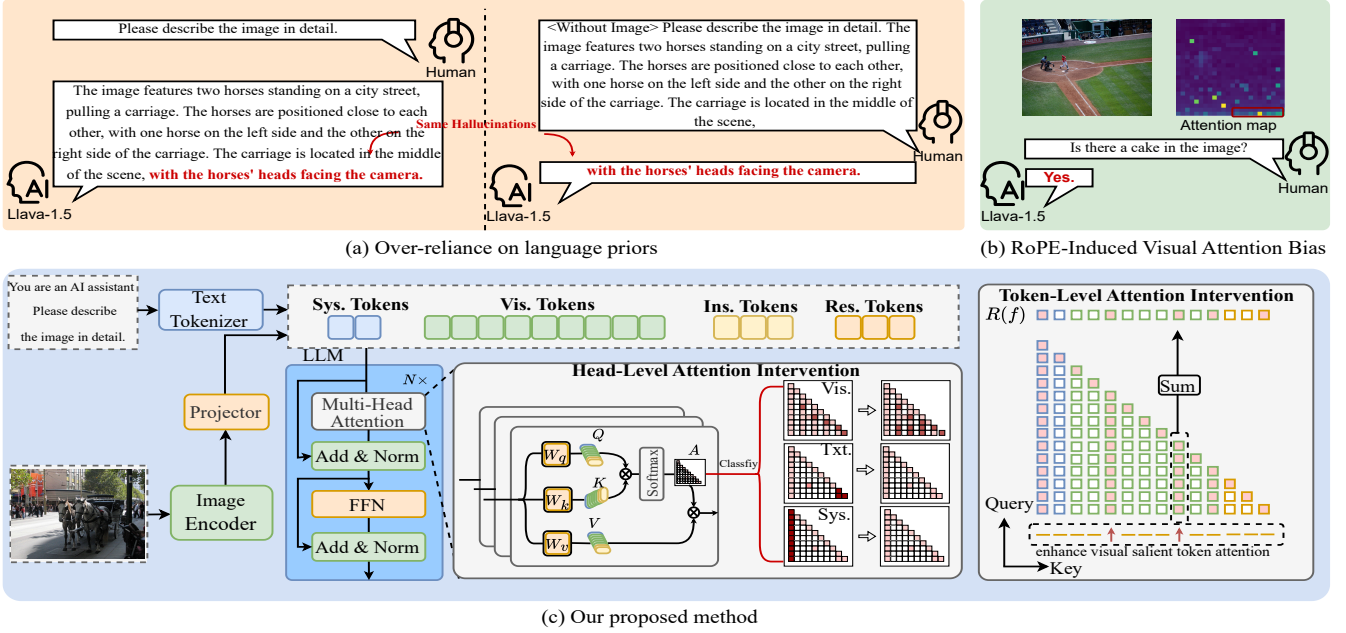


Figure 2: Overview of Visual Hallucination Causes and Our Solution: (a) Linguistic Over-reliance: hallucinations caused by excessive dependence on language priors; (b) RoPE-induced Attention Bias: attention skewed toward image tokens near text tokens due to positional proximity; (c) Our Method: mitigates these issues via Token-level Attention Intervention (TAI) to enhance focus on salient visual cues, and Head-level Attention Intervention (HAI) to suppress over-attention to system and nearby text tokens.

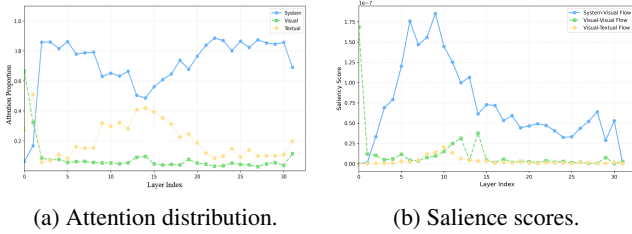


Figure 3: Layer-wise analysis of token attention distribution and cross-modal information flow in the decoder.

the aggregate information transfer from tokens in group \mathcal{B} to tokens in group \mathcal{A} , and can be instantiated with saliency, gradient-based relevance, or attention weight as $I(i, j)$.

We analyze the interaction strength among three token types across decoder layers using attention weights and saliency scores. Figures 3a and 3b respectively show the attention distributions and saliency scores, highlighting the prominent role of system-visual information flow in influencing predictions.

Token-Level Attention Intervention

Visual Sink and Salient Token Identification. To alleviate insufficient or misaligned visual attention—partly caused by RoPE-induced position bias—we identify visual-salient tokens that are important yet text-irrelevant. Formally, in each transformer decoder block, the attention matrix \mathbf{A} estimates

token relevance and reweights the value matrix \mathbf{V} to produce the output \mathbf{O} . We analyze intra-visual attention patterns to locate such salient tokens and enhance instruction-token attention toward them.

$$\mathbf{O} = \mathbf{A} \cdot \mathbf{V}, \quad (4)$$

$$\mathbf{A} = \text{Softmax} \left(\frac{\mathbf{Q}\mathbf{K}^\top}{\sqrt{d}} + \mathbf{M} \right) \quad (5)$$

where d is the dimensionality of query/key vectors, and $\mathbf{M} \in \mathbb{R}^{1 \times 1 \times n \times n}$ is the causal mask applied before the softmax operation. The attention matrix $\mathbf{A} \in \mathbb{R}^{b \times h \times n \times n}$ represents the attention weights, where b is the batch size, h is the number of attention heads, and n is the sequence length.

We define Intra-Visual Salient Token as visual tokens that receive excessive aggregated attention from other visual tokens while not contributing significantly to downstream alignment with textual outputs.

Let \mathcal{I}_{vis} denote the index set of all visual tokens, and let $\mathbf{A}_\ell^{(h)}$ represent the attention matrix of head h in decoder layer ℓ . We define the *reception score* $R(j)$ of a visual token $j \in \mathcal{I}_{\text{vis}}$ as the total amount of attention it receives from other visual tokens across all attention heads and decoder layers. Figure 4 visualizes the distribution of intra-visual reception scores $R(j)$ across decoder layers, revealing the uneven patterns of attention reception among visual tokens.

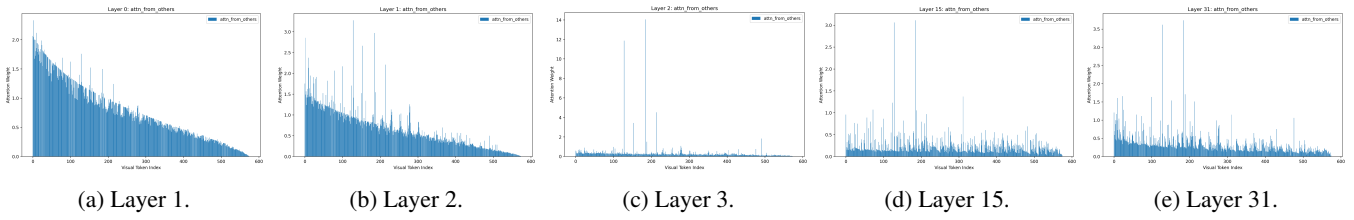


Figure 4: Visualization of intra-visual reception score $R(j)$ among visual tokens across decoder Layers.

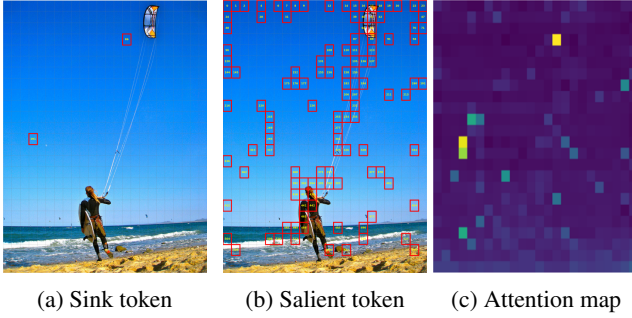


Figure 5: Visualization of visual attention in LLaVA-1.5-7B. (a) Visual Sink Token: tokens that absorbs much attention but lacks semantic contribution; (b) Visual Salient Token: tokens that aligns with meaningful visual regions critical for grounding; (c) Attention distribution over visual tokens.

$$R(j) = \frac{1}{H} \sum_{h=1}^H \sum_{i \in \mathcal{I}_{\text{vis}} \setminus \{j\}} \mathbf{A}_\ell^{(h)}[i, j], \quad (6)$$

where H is the total number of attention heads in the layer. Tokens with high reception scores are grouped into the following set:

$$\mathcal{I}_{\text{thres}}(\tau) = \left\{ j \in \mathcal{I}_{\text{vis}} \mid R(j) > \tau \cdot \max_{k \in \mathcal{I}_{\text{vis}}} R(k) \right\}, \quad (7)$$

We define a thresholded set of visual tokens $\mathcal{I}_{\text{thres}}^\ell(\tau)$ based on their relative attention scores $R(j)$, where a higher threshold $\tau = \frac{1}{2}$ identifies *sink tokens* and a lower threshold $\tau = \frac{1}{20}$ identifies *salient tokens*. As illustrated in Figure 5, we visualize the identified sink and salient tokens for a given image, alongside the full attention map, to highlight the discrepancy between attention magnitude and visual relevance.

Enhance Intra-Visual Salient Token Attention. To alleviate insufficient visual grounding and suppress anomalous attention patterns introduced by RoPE encoding, we intervene in the attention weights from instruction tokens ($i \in \mathcal{I}_{\text{ins}}$) to visual tokens ($j \in \mathcal{I}_{\text{vis}}$) in each decoder layer ℓ and head h by amplifying attention toward salient regions while suppressing semantically meaningless sink tokens. Formally, the adjusted attention weights are defined as:

$$A_{i,j}^{\ell,h} = \begin{cases} k \cdot A_{i,j}^{\ell,h}, & \text{if } j \in \mathcal{I}_{\text{salient}}^\ell \\ \delta \cdot A_{i,j}^{\ell,h}, & \text{if } j \in \mathcal{I}_{\text{sink}}^\ell \\ A_{i,j}^{\ell,h}, & \text{otherwise} \end{cases} \quad (8)$$

Here, $k > 1$ is a scaling factor used to strengthen attention toward salient visual tokens, and $\delta < 1$ is a decay factor that suppresses attention toward sink tokens.

After these adjustments, attention weights are re-normalized to ensure they remain a valid probability distribution:

$$A_{i,j}^{\ell,h} = \frac{A_{i,j}^{\ell,h}}{\sum_j A_{i,j}^{\ell,h}}, \quad \text{if } i \in \mathcal{I}_{\text{txt}} \quad (9)$$

This strategy encourages the model to aggregate more critical and reliable visual evidence while suppressing spurious focus on uninformative tokens.

Head-Level Attention Intervention

Prior studies (Musat 2024; Sun et al. 2024; Tang et al. 2025) have demonstrated that attention heads in large models often assume distinct functional roles. To investigate how different types of tokens influence decoder behavior in vision-language models, we categorize attention heads into three functional types: (1) **Visual-sensitive heads**, which focus strongly on visual tokens; (2) **System-prompt dominant heads**, which attend excessively to system prompt tokens; and (3) **Text-following heads**, which primarily follow instruction and response tokens. We then analyze how these head types are distributed across decoder layers to better understand the modality-specific flow of information.

Identifying Visual-Sensitive Heads. For each attention head h in decoder layer ℓ , we quantify its attention toward visual tokens as:

$$A_{\text{vis}}^{\ell,h} = \sum_{i \in \mathcal{I}_{\text{txt}}} \sum_{j \in \mathcal{I}_{\text{vis}}} \mathbf{A}^{\ell,h}[i, j], \quad (10)$$

where \mathcal{I}_{txt} denotes the set of instruction tokens during the prefill stage and the generated tokens during the decode stage. A head is considered visual-sensitive if its visual attention exceeds a significance threshold:

$$\mathcal{H}_{\text{vis}}^\ell = \left\{ h \mid A_{\text{vis}}^{\ell,h} > \mu + \lambda_{\text{vis}} \cdot \sigma \right\}, \quad (11)$$

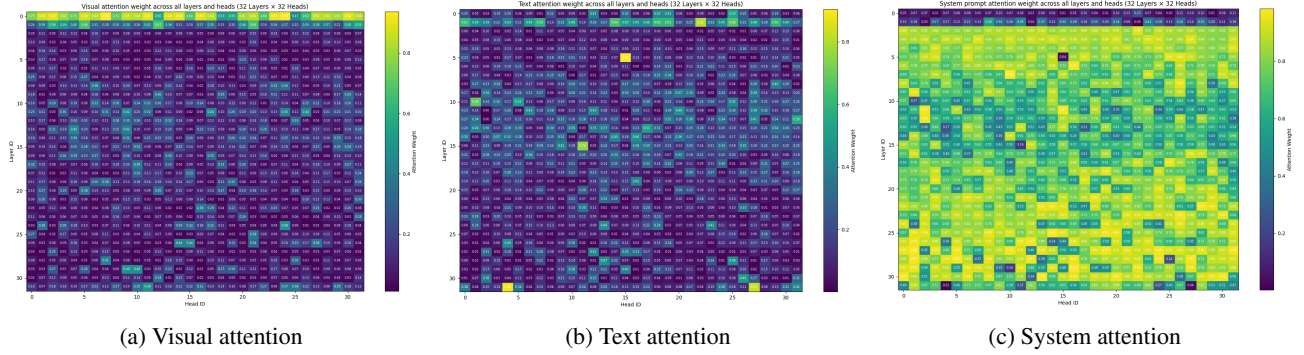


Figure 6: Layer-wise heatmaps of attention weights across all heads, showing preference for visual, text, and system tokens.

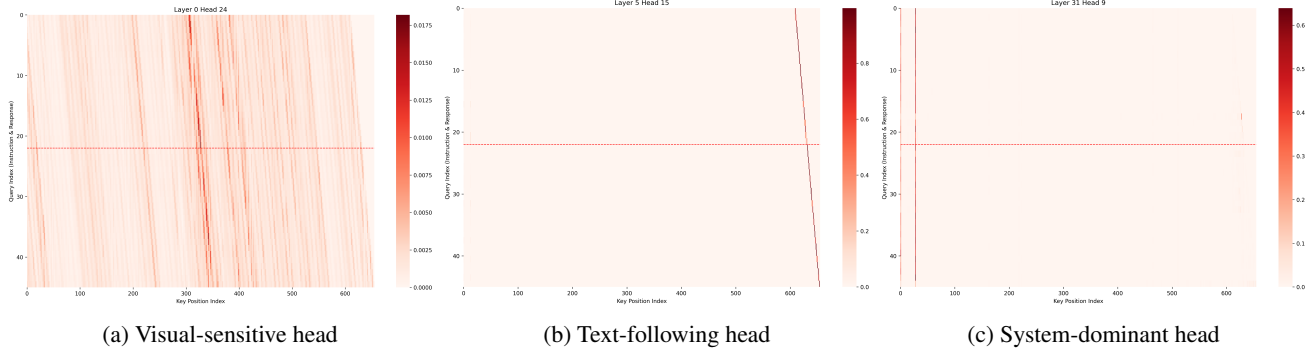


Figure 7: Attention maps from representative heads across modalities. Attention is visualized from instruction tokens (prefill) and response tokens (decode) to all key tokens. Red line separates the two phases.

where μ and σ are the mean and standard deviation of $A_{\text{vis}}^{\ell,h}$ across all heads in layer ℓ , and λ_{vis} is a tunable hyperparameter controlling sensitivity. This selection identifies heads that exhibit unusually strong attention toward visual input.

Identifying Text-Following Heads. Similarly, we compute attention directed toward textual tokens—specifically instruction and response tokens:

$$A_{\text{txt}}^{\ell,h} = \sum_{i \in \mathcal{I}_{\text{txt}}} \sum_{j \in \mathcal{I}_{\text{txt}}} \mathbf{A}^{\ell,h}[i, j], \quad (12)$$

Text-following heads are identified using a threshold λ_{txt} :

$$\mathcal{H}_{\text{txt}}^{\ell} = \left\{ h \mid A_{\text{txt}}^{\ell,h} > \lambda_{\text{txt}} \right\}. \quad (13)$$

where \mathcal{I}_{txt} indexes text tokens after the image (including instruction and response tokens), and λ_{txt} is a threshold.

Identifying System Prompt Dominant Heads. For each head h in layer ℓ , we compute its attention mass toward system prompt tokens:

$$A_{\text{sys}}^{\ell,h} = \sum_{i \in \mathcal{I}_{\text{txt}}} \sum_{j \in \mathcal{I}_{\text{sys}}} \mathbf{A}^{\ell,h}[i, j], \quad (14)$$

where \mathcal{I}_{sys} denotes the set of system prompt token indices. We then define the set of system prompt dominant heads as:

$$\mathcal{H}_{\text{sys}}^{\ell} = \left\{ h \mid A_{\text{sys}}^{\ell,h} > \lambda_{\text{sys}} \right\}, \quad (15)$$

where λ_{sys} is a predefined threshold controlling the sensitivity to identify system heads.

we validate the functionality of our defined three attention head types by zeroing out their weights. This classification framework lays the foundation for Head-level Attention Intervention (HAI) to suppress over-attention to system prompt tokens and text tokens introduced next.

Suppressing Over-Attention to the closest text tokens in Text Heads. we observe that certain attention heads predominantly focus on neighboring textual tokens, which may lead to early decisions based solely on linguistic priors. This behavior limits the model’s ability to incorporate visual cues. To alleviate this issue, we suppress the over-attention patterns of these *text heads* in the shallow layers of the decoder to encourage more balanced cross-modal fusion.

Suppressing Over-Attention to system tokens in System Heads. We also find that specific attention heads exhibit persistent attention to system prompt tokens throughout the generation process. Such behavior, often seen in *system heads*, may overly anchor generation on initial instructions, potentially obstructing downstream multimodal reasoning. We thus introduce a suppression strategy to mitigate this attention bias.

Unified Suppression Mechanism. To address both issues above, we apply a unified intervention strategy by directly

modulating the attention weights. Specifically, the attention output $\mathbf{A}_{l,h}$ from layer l and head h is adjusted as follows:

$$\tilde{\mathbf{A}}_{l,h}(i,j) = \begin{cases} (1 - \alpha_{\text{txt}}) \cdot \mathbf{A}_{l,h}(i,j), & \text{if } h \in \mathcal{H}_{\text{text}}, j \in \mathcal{I}_{\text{text}} \\ (1 - \alpha_{\text{sys}}) \cdot \mathbf{A}_{l,h}(i,j), & \text{if } h \in \mathcal{H}_{\text{sys}}, j \in \mathcal{I}_{\text{sys}} \\ \mathbf{A}_{l,h}(i,j), & \text{otherwise} \end{cases} \quad (16)$$

$$\hat{\mathbf{A}}_{l,h}(i,:) = \frac{\tilde{\mathbf{A}}_{l,h}(i,:)}{\sum_j \tilde{\mathbf{A}}_{l,h}(i,j)} \quad (17)$$

where α_{txt} and α_{sys} denote the suppression strengths for text and system tokens, which determine how much their attention is attenuated.

Experiments

Experimental Setup

We implement VISFLOW using greedy decoding (beam size 1, max length 64) and run all experiments on 8 NVIDIA RTX 4090 GPUs. For POPE, we set $k = 20$, $\delta = 0$, $\lambda_{\text{vis}} = 1$, $\lambda_{\text{sys}} = 0.8$, $\lambda_{\text{txt}} = 0.3$, $\alpha_{\text{sys}} = 0.6$ and $\alpha_{\text{txt}} = 1$. All baselines follow their default configurations to ensure a fair comparison. To ensure efficiency, attention head types are identified once during the *prefill* stage and reused throughout decoding. TAI is applied from the second decoder layer onward, while HAI is applied to all layers for system heads and limited to layers 0–7 for text heads. This unified intervention strategy ensures minimal overhead while effectively enhancing visual-text alignment and suppressing over-attention to prompt tokens. For MiniGPT-4 and mPLUG-Owl2, since their visual tokens are semantically compressed, TAI is not applied.

Main Results

We conduct comprehensive evaluations of VisFlow on three widely-adopted benchmarks: CHAIR (Rohrbach et al. 2018), POPE (Li et al. 2023b). These benchmarks respectively assess visual factuality, grounding robustness, and multimodal reasoning capabilities. Experimental results confirm that VisFlow consistently enhances the performance of large vision-language models across diverse tasks, demonstrating both its effectiveness and generalizability.

On the CHAIR benchmark, which evaluates visual grounding quality on the MSCOCO dataset (Lin et al. 2014), as shown in Table 1, VisFlow achieves substantially lower sentence-level hallucination rates CHAIR_s and instance-level hallucination rates CHAIR_i compared to existing decoding-based approaches such as VCD (Leng et al. 2024), DoLa (Chuang et al. 2023), and OPERA (Huang et al. 2024), indicating improved alignment between generated descriptions and visual content.

For the POPE benchmark, As shown in Table 2, VisFlow obtains the highest F1 scores across Random, Popular, and Adversarial subsets. The performance improvements are especially significant under the Adversarial setting, underscoring VisFlow’s capability to mitigate spurious correlations.

More Analysis and Ablation Experiments

Sensitivity of Hyper-parameters. To identify the optimal enhancement strength, we conduct an ablation study on the scaling factor k for salient visual tokens. As shown in Figure 8, the instance-level hallucination metric (CHAIR_i) exhibits a U-shaped trend with respect to k . The hallucination rate is minimized when $k = 20$, indicating the model benefits most from moderate reinforcement of attention to salient visual cues. Over-amplification (e.g., $k = 24$) or under-amplification ($k = 1$, i.e., baseline) leads to suboptimal performance, highlighting the importance of balanced visual emphasis.

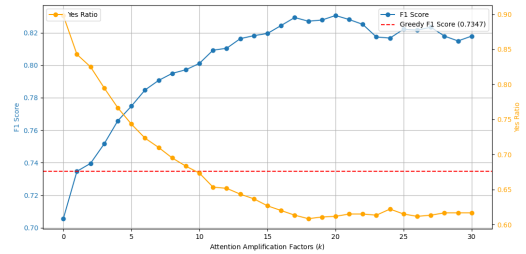


Figure 8: Performance on POPE (adv.): enhancing Salient Token Attention with different enhancement factor (k).

Functional Analysis of Attention Heads. To validate the functional roles of the three types of attention heads, we first identified the top-4 heads for each type based on their cumulative attention weights over visual, system, and text tokens, respectively. We then performed a causal intervention by zeroing out the attention weights of each selected group and evaluated the impact on model performance on CHAIR.

As shown in Table 4, masking visual-sensitive heads significantly increases CHAIR scores, confirming their importance for visual grounding. In contrast, Figure 9a and Figure 9b illustrate causal interventions on POPE by masking attention heads from different decoder layers, with thresholds $\lambda_{\text{sys}} = 0.7$ and $\lambda_{\text{txt}} = 0.3$. Masking text-following heads reduces hallucinations while masking System-prompt dominant heads, has minimal effect and can even reduce hallucinations indicating potential redundancy.

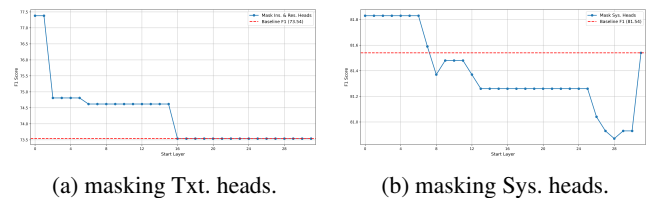


Figure 9: Ablation on head masking starting from different layers (l): (a) text heads on POPE (adversarial); (b) system heads on POPE (random).

Table 1: Comparison of CHAIR and Recall scores on the MSCOCO dataset. Our method significantly reduces hallucinations while improving object recall, demonstrating superior visual grounding. Results are averaged over five random runs.

Methods	LLaVA-1.5			MiniGPT-4			mPLUG-Owl2		
	CHAIR _i ↓	CHAIR _s ↓	Recall ↑	CHAIR _i ↓	CHAIR _s ↓	Recall ↑	CHAIR _i ↓	CHAIR _s ↓	Recall ↑
Greedy	20.1	6.9	59.0	25.0	9.2	58.7	23.0	9.6	54.4
Beam Search	20.0	6.5	57.0	24.0	9.2	56.7	18.0	6.4	53.0
OPERA	17.0	6.3	56.7	20.0	8.2	58.1	16.0	5.8	54.0
VCD	20.0	6.9	57.0	23.0	8.9	56.4	18.0	6.4	53.0
DoLa	19.0	6.5	57.0	19.0	8.1	56.3	18.0	6.1	53.0
Ours	15.0	3.8	63.1	18.0	7.8	56.3	16.0	4.9	53.5

Table 2: Comparison of F1 scores on the POPE benchmark under three evaluation settings: Random, Popular, and Adversarial. Our method consistently achieves the best performance across all scenarios and backbones, highlighting its robustness in grounding visual evidence. Results are averaged over five random runs.

Methods	LLaVA-1.5			MiniGPT-4			mPLUG-Owl2		
	Random ↑	Popular ↑	Adversarial ↑	Random ↑	Popular ↑	Adversarial ↑	Random ↑	Popular ↑	Adversarial ↑
Greedy	81.54	76.53	73.54	77.56	67.50	69.11	83.90	77.30	74.82
Beam Search	82.64	79.34	78.15	78.54	70.20	71.62	87.33	81.42	78.95
OPERA	79.50	76.63	75.88	78.35	69.65	71.42	87.03	80.29	77.92
VCD	82.51	79.33	78.17	78.61	69.95	71.62	87.36	81.42	78.95
DoLa	82.81	79.47	78.36	80.23	73.00	73.23	87.90	81.53	79.18
Ours	89.55	87.09	84.35	80.86	73.61	73.94	88.72	82.19	80.17

Table 3: Ablation Study on CHAIR Benchmark

Settings	CHAIR _s ↓	CHAIR _i ↓	Recall ↑	Length
Greedy (Baseline)	20.1	6.9	59.0	54.88
w/o TAI	16.0	4.8	56.7	55.12
w/o HAI	16.0	5.3	58.4	54.76
w/o HAI for Txt. Heads	18.0	6.4	61.1	54.25
w/o HAI for Sys. Heads	12.0	4.0	60.1	55.35
Our Full VisFlow	15.0	3.8	63.1	55.57

Table 4: Masking different type of Heads on CHAIR

Setting	CHAIR _s ↓	CHAIR _i ↓	Recall ↑	Length
Greedy (Baseline)	20.1	6.9	59.0	54.88
Mask Visual Heads	46.0	22.1	56.4	56.21
Mask System Heads	20.0	6.7	57.0	54.50
Mask Text Heads	19.0	7.2	58.4	53.88
Mask Random Heads	20.0	7.4	56.0	54.14

Decoding efficiency analysis

We evaluate the inference efficiency of our method by comparing it with several baseline approaches in terms of tokens per second (TPS) during decoding on CHAIR Benchmark, as shown in Figure 10. Our approach eliminates the need for iterative decoding or post-processing, making it substantially faster than contrastive methods while maintaining comparable latency to beam search.

Conclusion

In this paper, we tackle two main causes of visual hallucination in large vision-language models: Insufficient and erroneous visual perception, along with over-reliance

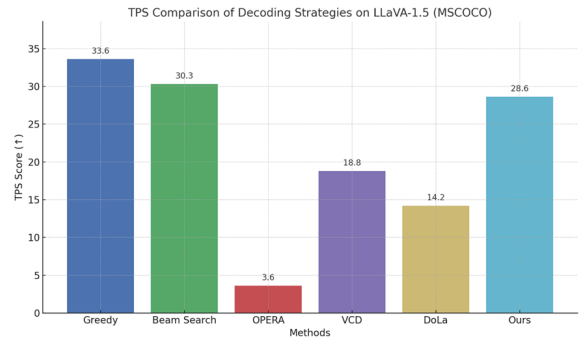


Figure 10: Comparison of our method with different baselines in terms of tokens per second (TPS) during decoding on CHAIR Benchmark.

on language priors. We propose VisFlow, a training-free, inference-time framework that reduces hallucinations by manipulating attention flows. Through attention analysis, we identify two critical types of visual tokens: visual sink tokens, which receive abnormally high and consistent attention from other visual tokens, and visual silence tokens, which are highly attended to by a broad range of tokens, alongside three pathological attention head types: visual heads, text heads, and system heads. To address these issues, we design TAI to enhance attention to visual silence tokens while suppressing attention to visual sink tokens, and HAI to suppress over-attention to system prompts and nearby text tokens. Extensive experiments on three benchmarks validate VisFlow’s effectiveness.

References

- An, W.; Tian, F.; Leng, S.; Nie, J.; Lin, H.; Wang, Q.; Dai, G.; Chen, P.; and Lu, S. 2024. Agla: Mitigating object hallucinations in large vision-language models with assembly of global and local attention. *arXiv preprint arXiv:2406.12718*.
- Bai, J.; Bai, S.; Yang, S.; Wang, S.; Tan, S.; Wang, P.; Lin, J.; Zhou, C.; and Zhou, J. 2023. Qwen-vl: A frontier large vision-language model with versatile abilities. *arXiv preprint arXiv:2308.12966*, 1(2): 3.
- Chen, J.; Zhu, D.; Shen, X.; Li, X.; Liu, Z.; Zhang, P.; Krishnamoorthi, R.; Chandra, V.; Xiong, Y.; and Elhoseiny, M. 2023a. Minigt-v2: large language model as a unified interface for vision-language multi-task learning. *arXiv preprint arXiv:2310.09478*.
- Chen, K.; Zhang, Z.; Zeng, W.; Zhang, R.; Zhu, F.; and Zhao, R. 2023b. Shikra: Unleashing Multimodal LLM's Referential Dialogue Magic. *ArXiv*, abs/2306.15195.
- Chen, Z.; Wu, J.; Wang, W.; Su, W.; Chen, G.; Xing, S.; Zhong, M.; Zhang, Q.; Zhu, X.; Lu, L.; et al. 2024a. Internvl: Scaling up vision foundation models and aligning for generic visual-linguistic tasks. In *Proceedings of the IEEE/CVF conference on computer vision and pattern recognition*, 24185–24198.
- Chen, Z.; Zhao, Z.; Luo, H.; Yao, H.; Li, B.; and Zhou, J. 2024b. Halc: Object hallucination reduction via adaptive focal-contrast decoding. *arXiv preprint arXiv:2403.00425*.
- Chiang, W.-L.; Li, Z.; et al. 2023. Vicuna: An Open-Source Chatbot Impressing GPT-4 with 90%* ChatGPT Quality. <https://vicuna.lmsys.org>. Accessed: April 14, 2023.
- Chuang, Y.-S.; Xie, Y.; Luo, H.; Kim, Y.; Glass, J.; and He, P. 2023. Dola: Decoding by contrasting layers improves factuality in large language models. *arXiv preprint arXiv:2309.03883*.
- Gunjal, A.; Yin, J.; and Bas, E. 2024. Detecting and preventing hallucinations in large vision language models. In *Proceedings of the AAAI Conference on Artificial Intelligence*, volume 38, 18135–18143.
- Huang, Q.; Dong, X.; Zhang, P.; Wang, B.; He, C.; Wang, J.; Lin, D.; Zhang, W.; and Yu, N. 2024. Opera: Alleviating hallucination in multi-modal large language models via over-trust penalty and retrospection-allocation. In *Proceedings of the IEEE/CVF Conference on Computer Vision and Pattern Recognition*, 13418–13427.
- Jiang, C.; Xu, H.; Dong, M.; Chen, J.; Ye, W.; Yan, M.; Ye, Q.; Zhang, J.; Huang, F.; and Zhang, S. 2024. Hallucination augmented contrastive learning for multimodal large language model. In *Proceedings of the IEEE/CVF Conference on Computer Vision and Pattern Recognition*, 27036–27046.
- Leng, S.; Zhang, H.; Chen, G.; Li, X.; Lu, S.; Miao, C.; and Bing, L. 2024. Mitigating object hallucinations in large vision-language models through visual contrastive decoding. In *Proceedings of the IEEE/CVF Conference on Computer Vision and Pattern Recognition*, 13872–13882.
- Li, J.; Li, D.; Savarese, S.; and Hoi, S. 2023a. Blip-2: Bootstrapping language-image pre-training with frozen image encoders and large language models. In *International conference on machine learning*, 19730–19742. PMLR.
- Li, Y.; Du, Y.; Zhou, K.; Wang, J.; Zhao, W. X.; and Wen, J.-R. 2023b. Evaluating object hallucination in large vision-language models. *arXiv preprint arXiv:2305.10355*.
- Lin, T.-Y.; Maire, M.; Belongie, S.; Hays, J.; Perona, P.; Ramanan, D.; Dollár, P.; and Zitnick, C. L. 2014. Microsoft coco: Common objects in context. In *Computer vision—ECCV 2014: 13th European conference, zurich, Switzerland, September 6–12, 2014, proceedings, part v 13*, 740–755. Springer.
- Liu, H.; Li, C.; Li, Y.; and Lee, Y. J. 2024a. Improved baselines with visual instruction tuning. In *Proceedings of the IEEE/CVF Conference on Computer Vision and Pattern Recognition*, 26296–26306.
- Liu, H.; Li, C.; Wu, Q.; and Lee, Y. J. 2023. Visual instruction tuning. *Advances in neural information processing systems*, 36: 34892–34916.
- Liu, H.; Xue, W.; Chen, Y.; Chen, D.; Zhao, X.; Wang, K.; Hou, L.; Li, R.; and Peng, W. 2024b. A survey on hallucination in large vision-language models. *arXiv preprint arXiv:2402.00253*.
- Ma, F.; Jin, X.; Wang, H.; Xian, Y.; Feng, J.; and Yang, Y. 2024. Vista-llama: Reducing hallucination in video language models via equal distance to visual tokens. In *Proceedings of the IEEE/CVF Conference on Computer Vision and Pattern Recognition*, 13151–13160.
- Manakul, P.; Liusie, A.; and Gales, M. J. 2023. Self-checkgpt: Zero-resource black-box hallucination detection for generative large language models. *arXiv preprint arXiv:2303.08896*.
- Musat, T. 2024. Mechanism and Emergence of Stacked Attention Heads in Multi-Layer Transformers. *arXiv preprint arXiv:2411.12118*.
- Rohrbach, A.; Hendricks, L. A.; Burns, K.; Darrell, T.; and Saenko, K. 2018. Object hallucination in image captioning. *arXiv preprint arXiv:1809.02156*.
- Ru, J.; Xie, Y.; Zhuang, X.; Yin, Y.; and Zou, Y. 2025. Do we really have to filter out random noise in pre-training data for language models? *arXiv preprint arXiv:2502.06604*.
- Sarkar, P.; Ebrahimi, S.; Etemad, A.; Beirami, A.; Arık, S. Ö.; and Pfister, T. 2024. Data-augmented phrase-level alignment for mitigating object hallucination. *arXiv preprint arXiv:2405.18654*.
- Simonyan, K.; Vedaldi, A.; and Zisserman, A. 2013. Deep inside convolutional networks: Visualising image classification models and saliency maps. *arXiv preprint arXiv:1312.6034*.
- Sun, Z.; Zang, X.; Zheng, K.; Song, Y.; Xu, J.; Zhang, X.; Yu, W.; and Li, H. 2024. Redep: Detecting hallucination in retrieval-augmented generation via mechanistic interpretability. *arXiv preprint arXiv:2410.11414*.
- Tang, F.; Huang, Z.; Liu, C.; Sun, Q.; Yang, H.; and Lim, S.-N. 2025. Intervening anchor token: Decoding strategy

in alleviating hallucinations for MLLMs. In *The Thirteenth International Conference on Learning Representations*.

Touvron, H.; Lavril, T.; Izacard, G.; Martinet, X.; Lachaux, M.-A.; Lacroix, T.; Rozière, B.; Goyal, N.; Hambro, E.; Azhar, F.; et al. 2023. Llama: Open and efficient foundation language models. *arXiv preprint arXiv:2302.13971*.

Xing, Y.; Li, Y.; Laptev, I.; and Lu, S. 2024. Mitigating object hallucination via concentric causal attention. *Advances in Neural Information Processing Systems*, 37: 92012–92035.

Ye, Q.; Xu, H.; Ye, J.; Yan, M.; Hu, A.; Liu, H.; Qian, Q.; Zhang, J.; and Huang, F. 2024. mplug-owl2: Revolutionizing multi-modal large language model with modality collaboration. In *Proceedings of the IEEE/CVF conference on computer vision and pattern recognition*, 13040–13051.

Yin, S.; Fu, C.; Zhao, S.; Xu, T.; Wang, H.; Sui, D.; Shen, Y.; Li, K.; Sun, X.; and Chen, E. 2024. Woodpecker: Hallucination correction for multimodal large language models. *Science China Information Sciences*, 67(12): 220105.

Zhang, Z.; Yadav, S.; Han, F.; and Shutova, E. 2024. Cross-modal Information Flow in Multimodal Large Language Models. *arXiv preprint arXiv:2411.18620*.

Zhuang, X.; Xie, Y.; Deng, Y.; Liang, L.; Ru, J.; Yin, Y.; and Zou, Y. 2025a. VARGPT: Unified Understanding and Generation in a Visual Autoregressive Multimodal Large Language Model. *arXiv preprint arXiv:2501.12327*.

Zhuang, X.; Zhu, Z.; Chen, Z.; Xie, Y.; Liang, L.; and Zou, Y. 2024. Game on Tree: Visual Hallucination Mitigation via Coarse-to-Fine View Tree and Game Theory. In *Proceedings of the 2024 Conference on Empirical Methods in Natural Language Processing*, 17984–18003.

Zhuang, X.; Zhu, Z.; Xie, Y.; Liang, L.; and Zou, Y. 2025b. VASparse: Towards Efficient Visual Hallucination Mitigation for Large Vision-Language Model via Visual-Aware Sparsification. *arXiv preprint arXiv:2501.06553*.

Not All Tokens and Heads Are Equally Important: Dual-Level Attention Intervention for Hallucination Mitigation

LLaVA-1.5(Greedy):

The image features two horses standing on a city street, pulling a carriage. The horses are positioned close to each other, with one horse on the left side and the other on the right side of the carriage. The carriage is located in the middle of the scene, **with the horses' heads facing the camera**. There are several people in the background, some of them walking or standing near the horses and carriage. A few individuals are closer to the left side of the scene, while others are scattered around the right side. **A handbag can be seen near the center of the scene, possibly belonging to one of the pedestrians.**

Please describe the image in detail.



VCD:

The image depicts a city street scene with two horses pulling a carriage. The horses are positioned close to each other, with one horse on the left side and the other on the right side of the street. The carriage is located in the middle of the scene, with the horses harnessed to it. There are several people in the image, with some standing near the horses and others walking along the street. A few individuals can be seen in the background, while others are closer to the foreground. **A handbag is also visible in the scene, possibly belonging to one of the pedestrians.**

VisFlow:

The image features two horses pulling a carriage down a city street. The horses are positioned on the sidewalk, with one horse closer to the left side of the street and the other horse on the right side. The horses are wearing blinders, which are designed to protect their eyes from the bright sunlight. There are several people walking along the street, with some of them closer to the horses and others further away. A few of the people are carrying handbags, indicating that they might be tourists or locals out for a stroll.

LLaVA-1.5(Greedy):

The image features a white toilet with a green seat, situated in a bathroom. The toilet is positioned under a sink, which is located on the left side of the bathroom. **Above the toilet, there is a mirror, and a towel is hanging on the right side of the bathroom. In addition to the toilet, there is a bottle placed on the right side of the bathroom, and a cup can be seen on the left side.** The bathroom appears to be well-maintained and clean, with a focus on the white toilet and green seat.

Please describe the image in detail.



VCD:

The image depicts a clean and well-organized bathroom featuring a white toilet situated next to a walk-in shower. **The shower has a glass door, and there is a wooden cabinet above the toilet. The bathroom also includes a sink with a mirror above it, and a towel rack is placed nearby.** In addition to the main bathroom fixtures, **there are a couple of bottles placed on the countertop, and a pair of scissors can be seen resting on the edge of the sink.** The overall appearance of the bathroom is tidy.

VisFlow:

The image features a white toilet with a green seat. The toilet is situated in a bathroom, and is the main focus of the scene. The toilet is clean and ready for use. The bathroom is equipped with a sink, which is located to the left of the toilet. The sink is also clean and ready for use. The bathroom is well-maintained and ready for use.

LLaVA-1.5(Greedy):

The image features a group of **four** horses grazing on grass in a field. They are spread out across the scene, with one horse on the left side, another in the middle, and **two** more on the right side. The horses are peacefully eating the grass, enjoying their time in the open field. In the background, there is a yellow sign with an arrow pointing to the right, possibly indicating a direction or a nearby location. The scene is set against a backdrop of trees, creating a serene and natural atmosphere.

Please describe the image in detail.



VCD:

The image depicts a group of **four** horses grazing in a grassy field. The horses are spread out across the field, with one horse on the left side, another in the middle, and **two** more on the right side. They are all focused on eating the grass, enjoying their time in the open field. In the background, there is a yellow sign with an arrow pointing to the right, possibly indicating the direction to a nearby location or trail. The scene is set against a backdrop of trees, creating a peaceful and natural atmosphere.

VisFlow:

The image features a group of horses grazing in a field. There are three horses in the scene, with one horse on the left side, another in the middle, and the third horse on the right side. The horses are eating grass in a field, with a yellow sign in the background. The sign is pointing to the right, indicating the direction of the road. The scene is set in a forest with trees surrounding the area.

Figure 11: VisFlow's performance on reducing hallucinations of LLaVA-1.5-7B.